Complex Nanoparticles Based on Chitosan and Ionic/Nonionic Strong Polyanions: Formation, Stability, and Application

Ecaterina Stela Dragan* and Marcela Mihai†

"Petru Poni" Institute of Macromolecular Chemistry, Aleea Grigore Ghica Voda 41 A, RO-700487 Iasi, Romania

Simona Schwarz‡

Leibniz Institute of Polymer Research, Hohe Strasse 6, 01069 Dresden, Germany

ABSTRACT Interpolyelectrolyte complex (IPEC) nanoparticles formed between chitosan having different molar masses (470, 670, and 780 kDa) and two random copolymers of 2-(acrylamido)-2-methylpropanesulfonate (AMPS) with *tert*-butylacrylamide (TBA) [P($AMPS_{54}$-*co*-TBA_{46}) and P($AMPS_{37}$-*co*-TBA_{63})] were prepared by the dropwise addition of polyanion onto the chitosan solution. The effect of polyelectrolyte characteristics and the molar ratio between charges on the morphology of the complex nanoparticles and on their colloidal stability was deeply investigated by turbidimetric titration (optical density at 500 nm), dynamic light scattering, and atomic force microscopy. It was found that the lowest sizes of the IPEC nanoparticles were obtained, with both polyanions, when the chitosan having the lowest molar mass (470 kDa) was used as a major component. In this case, the particle sizes varied in a narrow range, even after the complex stoichiometry; i.e., when the polyanion was added in excess, the colloidal stability of these IPEC dispersions was very high. A mechanism of complex formation as a function of the ratio between charges was proposed. According to this mechanism, the nonstoichiometric complex nanoparticles formed at molar ratios between charges, n^-/n^+, lower than 0.2, i.e., far from the complex stoichiometry, would have a high density of positive charges in excess not only because of the chitosan in excess, which forms the shell, but also because of the mismatch of opposite charges, due to both the differences in the flexibility of complementary polyions and the presence of the hydrophobic comonomer, TBA, in the polyanion structure. Nonstoichiometric IPECs prepared at n^-/n^+ around 0.2 proved to be more efficient than chitosan in the destabilization of kaolin from a model suspension, with a lower optimum concentration flocculation and a much larger flocculation window being found compared with chitosan.

KEYWORDS: chitosan • anionic/nonionic copolymers • nonstoichiometric interpolyelectrolyte complex dispersions • dynamic light scattering • atomic force microscopy • kaolin

I. INTRODUCTION

Interpolyelectrolyte complexes (IPECs) attracted much interest, from the beginning, either as stoichiometric and insoluble materials or as nonstoichiometric complexes (1−3). Stoichiometric IPECs, characterized by an almost total compensation of opposite charges, are usually highly aggregated systems, formed by a "scrambled egg" mechanism (1, 4−6). Soluble nonstoichiometric IPECs (NIPECs) result mainly when the complementary polyelectrolytes have significantly different molar masses, with structural differences between polyions and the presence of low amounts of NaCl also being necessary (7−9). NIPECs as colloidal dispersions bearing free charges in excess (10−18) were mainly used for surface modification (11, 19, 20), or as nanocarriers for drugs, proteins, DNA, etc. (21, 22). The use of NIPEC dispersions for destabilization of solid−liquid systems is another attractive direction of application. It is well-known that the efficiency of a certain flocculant in separation processes is evaluated as a function of two main parameters: the optimum flocculation concentration, which should be as low as possible, and the flocculation window, which must be as large as possible (23). The most widely used polymeric flocculants are polycations because the majority of solid particles in suspensions have negative charges. However, polycations have a main drawback, which is the narrow flocculation window. An improvement of this aspect was brought by using NIPECs as colloidal dispersions bearing free positive charges in excess (12, 24, 25). So far, the optimum concentration of the complex required for flocculation was much higher than the optimum concentration of the polycation alone, even if the flocculation window was much larger with NIPECs. Therefore, a study of the factors that allow tuning of the complex properties to simultaneously fulfill both conditions is strongly required. Furthermore, the majority of synthetic flocculants are obtained from petroleum-based row materials by processing chemistry, which is not always environmentally friendly, with numerous contaminants arising in water from the residual unreacted monomers (26).

* Corresponding author. Tel.: +40.2322217454. Fax: +40.232211299. E-mail: sdragan@icmpp.ro.

Received for review February 19, 2009 and accepted April 25, 2009

† E-mail: marcelas@icmpp.ro.

‡ E-mail: simsch@ipfdd.de.

DOI: 10.1021/am900109u

Scheme 1. Chemical Structures of the Polyelectrolytes

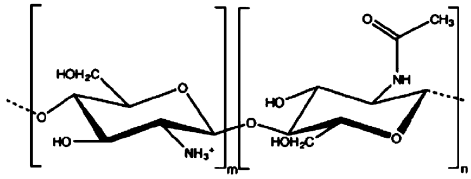

Chitosan

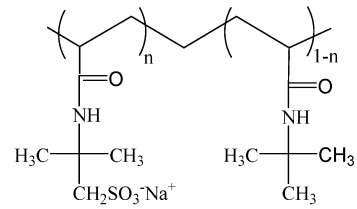

n = 54, P(AMPS$_{54}$-co-TBA$_{46}$)

n = 37, P(AMPS$_{37}$-co-TBA$_{63}$)

In this context, the ionic polymers coming from the renewable resources either as bioflocculants (12, 26) or as components of the IPECs (27−31) are gaining more and more attention. Chitosan, the linear cationic polysaccharide composed of β-(1→4)-2-amino-2-deoxy-D-glucopyranose and β-(1→4)-2-acetamido-2-deoxy-D-glucopyranose units randomly distributed along the polymer chain, has attracted numerous scientists because of its outstanding biological properties like biodegradability, biocompatibility, and antibacterial activity (26). Chitosan has been extensively used either alone in pharmaceutical systems, medicine, cosmetics, food, agriculture, and wastewater treatment (32−36) or as IPECs formed with synthetic (37−40) and natural polyanions (41−44). It has already been shown that the IPECs based on chitosan, by virtue of their biocompatibility, have valuable biomedical applications such as membranes for dialysis, packaging, coatings and wound dressing, and polyelectrolyte complex beads for controlled delivery of proteins, drugs, and vaccines (45−52).

Although the IPECs of chitosan with some polyanions, mainly homopolymers, have been studied (38−40), finding the formation conditions of novel chitosan-based IPECs as colloidal dispersions and tailoring their properties for certain applications are still challenges. It was found that the ionic/nonionic copolymers (53, 54) allow tuning of the complex properties by both the charge density and the hydrophilic/hydrophobic balance, but, so far, the studies were focused mainly on the IPECs formed with synthetic polycations. Furthermore, the presence of stimuli-responsive comonomers recommends such copolymers as components in the preparation of novel "smart" materials, with the stimuli-responsive IPECs being promising for controlled-release systems, on−off switchers, ecology, and so on (21, 55, 56).

Therefore, the objective of the present work was focused on the formation and properties of some IPECs as colloidal dispersions based on chitosan with different molar masses and two ionic/nonionic random copolymers of 2-(acrylamido)-2-methylpropanesulfonate (AMPS) with *tert*-butylacrylamide (TBA), P(AMPS$_{37}$-*co*-TBA$_{63}$) and P(AMPS$_{54}$-*co*-TBA$_{46}$). To the best of our knowledge, this is the first systematic study of the morphology and colloidal stability of the IPEC nanoparticles elaborated by using ionic/nonionic random copolymers of AMPS with TBA as strong polyanions and chitosan as the polycation, with special attention being given to the mechanism of the complex formation, when chitosan was the major component, and to the influence of the noionic comonomer content and the molar ratio between charges on the efficiency of the chitosan-based NIPECs in destabilization of a kaolin model dispersion. The acceptance by the U.S. Food and Drug Administration of the copolymers of TBA with various acrylic comonomers as indirect additives (57) and their recognized temperature-responsive properties (58, 59) would be also of interest for future applications of the IPEC nanoparticles formed with chitosan.

Table 1. Some Characteristics of Oppositely Charged Polyions

sample code	η, mPa s	$[\eta]$, dL/g	M_v, kDa	M_u,[a] g/charge	b,[b] nm
ChI	400	9.12[c]	470	196.8	0.643
ChII	800	12.33[c]	670	196.8	0.643
ChIII	1000	14.07[c]	780	196.8	0.643
P(AMPS$_{54}$-*co*-TBA$_{46}$)		0.33[d]	175	337.0	0.463
P(AMPS$_{37}$-*co*-TBA$_{63}$)		0.47[d]		440.6	0.667

[a] Mass per charge. [b] Distance between charges. [c] In 0.3 M CH_3COOH/0.2 M CH_3COONa (1:1, v/v), at 25 °C. [d] In 1 M NaCl, at 25 °C.

II. MATERIALS AND METHODS

II.1. Materials. The chemical structures of the polyelectrolytes used in this study are presented in Scheme 1, with some characteristics being summarized in Table 1.

Chitosan samples were purchased from Heppe GmbH (Biotechnologische Systeme und Materialien) as flakes, ash content less than 1%, and were used without further purification. The viscometric average molar masses of chitosan samples were estimated using eq 1 (60):

$$[\eta] = 1.38 \times 10^{-4} M_v^{0.85} \quad (1)$$

The intrinsic viscosity of a chitosan solution in 0.3 M CH_3COOH/0.2 M CH_3COONa (1:1, v/v) was measured with an Ubbelohde viscometer at 25 ± 0.1 °C.

The degree of acetylation (DA) of chitosans was evaluated by IR spectroscopy by using a Bruker Vertex 70 FT-IR spectrometer. Transmission spectra were recorded either in KBr pellets or in dry films (casted from 1% solutions in 1% acetic acid) using a standard sample holder. For the DA determination, a linear correlation proposed by Brugnerotto et al. (61) (eq 2) was used, taking the 1420 cm^{-1} band as the reference and the band located at 1320 cm^{-1} as the characteristic band for *N*-acetylglucosamine.

$$A_{1320}/A_{1420} = 0.3822 + 0.03133\mathrm{DA} \quad (2)$$

The medium value of DA = 20% for all chitosan samples was taken into account in this study.

Copolymers of AMPS with TBA were synthesized and purified according to ref 62.

Kaolin powder (from Aldrich) with particles of 350 nm was used as the model substrate for fine particles. The kaolin dispersions with a concentration of 1 g/L and pH 6 were prepared by ultrasonic treatment for 15 min followed by vigorous stirring for 1 h.

II.2. Preparation of Polyelectrolyte Solutions. The chitosan solutions with a concentration of 1 g/L were obtained by dissolving the flakes in a 1 vol % acetic acid solution with moderate stirring for at least 48 h. In order to use the chitosan solution for IPEC preparation, the concentration was adjusted to 0.5 mM by dilution into a 1 vol % acetic acid solution. Aqueous solutions of the anionic polyelectrolytes with a concentration of 5 mM were prepared by adequate dilution of the stock solutions (10 mM) with distilled water. The concentrations of both the chitosan and polyanion solutions were prepared by taking into account the molar mass of the repeat unit in g/charge; see Table 1. The concentration of the charged groups in all solutions was determined by a PCD 02 particle charge detector (Mütek GmbH, Herrsching, Germany). Before use, all solutions were adjusted at pH 4.0 with 0.1 M HCl for polyanions and 0.1 M NaOH for chitosan.

II.3. IPEC Preparation. Dispersions of IPECs were prepared at room temperature (about 25 °C), by mixing aqueous solutions of oppositely charged polyelectrolytes in appropriate proportions. The amount of chitosan was kept constant within a complex series, while the amount of polyanion was varied according to the desired mixing molar ratio, n^-/n^+. The polyanion was added dropwise to the polycation, under magnetic stirring, with a constant addition rate of 3.8 mL of polyanion/(mL of chitosan · h). After mixing, the dispersions formed were stirred 60 min and were characterized after 24 h, if other conditions were not specified.

II.4. Polyelectrolyte Titration. A quantitative determination of the polyelectrolyte in solution, the charge density, and the detection of the isoelectric point in the complex formation was performed by polyelectrolyte titration with a PCD 03 particle charge detector (Müteck GmbH, Herrsching, Germany) using either poly(sodium ethylenesulfonate) or poly(diallyldimethylammonium chloride), with a concentration of 10^{-3} mol/L, depending on the nature of the charges.

II.5. Turbidimetry. The turbidity of the complex dispersions was characterized by the optical density at $\lambda = 500$ nm (OD_{500}), with a Lambda 900 spectrometer (Perkin-Elmer, Cambridge, U.K.), using deionized water to establish the baseline. At this wavelength, the used polyelectrolytes do not absorb. Optical density results were expressed as the average of at least two independent measurements.

II.6. Dynamic Light Scattering (DLS). DLS is a technique used for particle sizing of samples, typically in the submicrometer range. The technique measures the time-dependent fluctuations in the intensity of scattered light from a suspension of particles undergoing random Brownian motion. Analysis of the time dependence of the intensity fluctuation can yield the *z*-average translational diffusion coefficient (D) of the particles from which, via the Stokes−Einstein equation (eq 3), when the viscosity of the medium is known, the hydrodynamic diameter, D_h, of the particles can be calculated (63).

$$D_h = k_B T/3\eta_s \pi D \quad (3)$$

where k_B is the Boltzmann constant, T is the absolute temperature (298 K), and η_s is the dynamic viscosity of the solvent (for water, 0.8872 cP).

To get information about the size distribution of PEC particles, the polydispersity index, PI, was also included in the interpretation. The autocorrelation function $g(\tau)$ was expanded in a power series (eq 4, methods of cumulants (63)):

$$g(\tau) = \exp[-\langle\Gamma\rangle\tau + (\mu_2/2)\tau^2 - (\mu_3/3!)\tau^3 + \ldots] \quad (4)$$

where τ is the correlator time delay and $\langle\Gamma\rangle$ is the mean reciprocal decay time. The second cumulant (μ_2) is a measure of the reciprocal decay time around the average value, allowing determination of PI (eq 5):

$$PI = \mu_2/\langle\Gamma\rangle^2 \quad (5)$$

The measurements were carried out using a Zetasizer 3000 (Malvern Instruments, Worcestershire, U.K.) equipped with a 10 mW He−Ne laser operating at $\lambda = 633$ nm, at a scattering angle of 90°. The samples were kept at a constant temperature of 25 °C during all experiments. The reported results are the average of two DLS-independent measurements.

II.7. Atomic Force Microscopy (AFM). Prior to use, the silicon wafer substrates were carefully cleaned in two steps: first, in a "piranha solution" followed by intensive rinsing with deionized water and, second, with the mixture NH_4OH/H_2O_2/deionized water, at 70 °C, in an ultrasonic bath, intensively rinsed with water, and finally dried under a nitrogen flow. The clean silicon wafer substrates were immersed in IPEC dispersions, identical with those used for DLS, for 20 min, then three times each 1 min in distilled water, and finally air-dried at room temperature (in a dust-free environment) for about 48 h. The shapes of the IPEC particles were examined by means of a Nanoscope IIIa Dimension 3100 scanning proton microprobe (Digital Instruments Veeco Metrology Group, Woodbury, NY). The topographic images were obtained in tapping mode and were repeated on different areas of the same sample. The IPEC particle sizes were determined using the *Particle Analysis* function of the device software, which is designed to detect and measure the lateral dimensions of isolated particles on the sample surfaces and to determine the minimum, maximum, and mean diameters for the analyzed particles. The sizes of about 50 individual IPEC particles adsorbed on the silicon substrate were measured directly from AFM topographic images, using the device software.

II.8. Destabilization of a Model Suspension with NIPEC Dispersions. Destabilization experiments were conducted at room temperature. Volumes of 50 mL of a kaolin model suspension were stirred at 120−150 rpm in beakers, and then different volumes of a chitosan solution or a NIPEC dispersion were added. Stirring was continued at the same speed for about 2 min, and then it was decreased to about 50 rpm for 15 min. After a settling time of about 20 min, the reading of OD_{500} was performed with a SPECORD M42. Deionized water was used as a reference. The residual turbidity (RT) was calculated with eq 6:

$$RT = (OD_{500s}/OD_{500i}) \times 100\% \quad (6)$$

where OD_{500s} was OD_{500} after the addition of a flocculant and OD_{500i} was OD_{500} of the initial model suspension.

III. RESULTS AND DISCUSSION

III.1. Formation and Characterization of IPEC Colloidal Dispersions. The physicochemical and biological properties of chitosan depend mainly on the fraction and

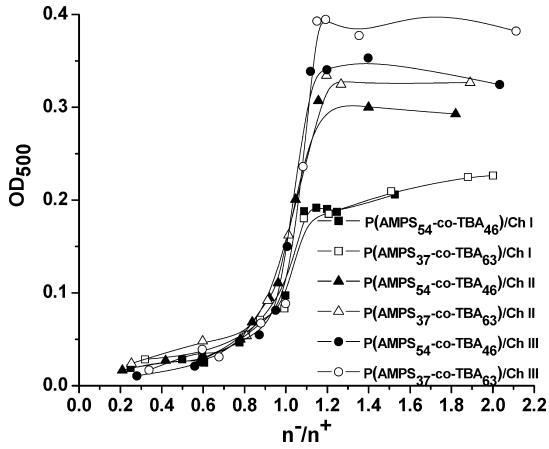

FIGURE 1. OD_{500} values as a function of the molar ratio between charges, n^-/n^+.

distribution of the two kinds of repeating units along the chains (glucosamine and *N*-acetylglucosamine), the pH of the solution, and the degree of polymerization (64−66). In our experiments, the initial solutions of polyelectrolytes were adjusted to pH 4.0. The deacetylation degree was about the same for all samples of chitosan; only the chitosan molar mass varied (Table 1). Because of the constant pH, the charge density of chitosan remained unchanged, whereas the charge density of polyanions was adjusted in the synthesis process. It was already demonstrated that the titrant addition rate is a valuable parameter in the control of the particle size, shape, and polydispersity (67, 68). A constant addition rate of 3.8 mL of polyanion/(mL of chitosan · h) was used because in our previous investigations, upon formation of IPECs as colloidal dispersions from synthetic polycations and polyanions, this was the optimum addition rate, taking into account the complex morphology, on the one hand, and the preparation speed, on the other hand (67, 68).

In a certain medium, the main characteristics of the IPEC particles (size, shape, and polydispersity) are governed by the structural parameters of the components such as their charge density, hydrophobicity, and chain length. Furthermore, the release of the corresponding small counterions contributes to the increase of the system entropy and thus to the complex stability.

The formation of colloidal IPECs between chitosan and P(AMPS$_{37}$-*co*-TBA$_{63}$) or P(AMPS$_{54}$-*co*-TBA$_{46}$) was followed first by turbidimetric titration, OD_{500}, as a function of the mixing ratio n^-/n^+, i.e., the molar ratio between anionic and cationic units (Figure 1).

The results presented in Figure 1 could be assigned mainly to the increase of the concentration of the complex nanoparticles and also to the changes in their sizes and polydispersities, with the turbidity being influenced by some intrinsic properties of the dispersion, such as the concentration (number), size, molar mass, and polydispersity of the particles (16, 43). The common feature for all studied systems was the slow increase of the turbidity up to a molar ratio, n^-/n^+, of about 0.8, with the OD_{500} values being a little higher when P(AMPS$_{37}$-*co*-TBA$_{63}$) was the added polyion compared to P(AMPS$_{54}$-*co*-TBA$_{46}$). The complex stoichiometry, indicated by an abrupt increase of the turbidity, was located at a ratio between charges of around 1:1, even if the complementary polyions used in the complex formation were different by strength [chitosan is a weak polycation but the P(AMPS-*co*-TBA) polymers are strong polyanions], flexibility (chitosan has a semirigid chain, unlike the synthetic polyanions, which are flexible), and molar mass. A strong influence of the chitosan molar mass on the OD_{500} values, after stoichiometry, was observed, with a clear influence of the polyanion structure being evident only for chitosan II and III, i.e., for larger differences between the polyion molar masses.

DLS was used as a more suitable method to monitor the peculiarities of the complex formation. As can be observed in Figure 2a, the particle sizes were strongly influenced by the polyion characteristics, on the whole range of the ratio between charges.

As a common trend, the particle sizes slowly decreased up to n^-/n^+ of about 0.8, remained almost unmodified up to n^-/n^+ of about 1.2, and abruptly increased after that, mainly when chitosan II and III were the starting polyions, with the particle sizes always being higher when P(AMPS$_{37}$-*co*-TBA$_{63}$) was the added polyion. The decrease in the particle sizes, before stoichiometry, suggests that when the polyanion is in default and chitosan is in excess, the addition of polyanion allows both the formation of new particles, evidenced by the slow increase of the OD_{500} values, and also their rearrangement toward more compact structures. The region of n^-/n^+ ranging from about 0.8 up to 1.2, characterized by an almost constant size of the complex particles, unlike the complexes formed from the same polyanions and synthetic polycations, which were characterized by an abrupt increase of the particle sizes after complex stoichiometry (68), seems to be a characteristic of the complexes formed between chitosan and the two random copolymers P(AMPS-*co*-TBA). As Figure 2a shows, the secondary aggregation of the particles took place after n^-/n^+ of about 1.2, leading to the monotonous increase of the complex particle sizes. This shows that the secondary aggregation was not as fast as that in the case of synthetic polycations, which are much more flexible than chitosan (67, 68), because of the high structural differences between the complementary polyions.

The polyanion charge density influenced the particle sizes both before and after stoichiometry. Thus, when P(AMPS$_{37}$-*co*-TBA$_{63}$) was used as the polyanion, the higher content of the nonionic and hydrophobic comonomer led to an increase of the polyanion amount required for charge compensation, with the particle sizes being always higher compared with the sizes of the IPECs formed with P(AMPS$_{54}$-*co*-TBA$_{46}$) as the polyanion.

Figure 2b shows that PI followed almost the same trend as the particle sizes, with the smallest values of PI being obtained at n^-/n^+ ranging from 0.8 to 1.2. A high polydispersity of the complex particles was reported for the IPECs formed between chitosan and dextran sulfate (43, 44), but the polydispersity was much lower when synthetic polyca-

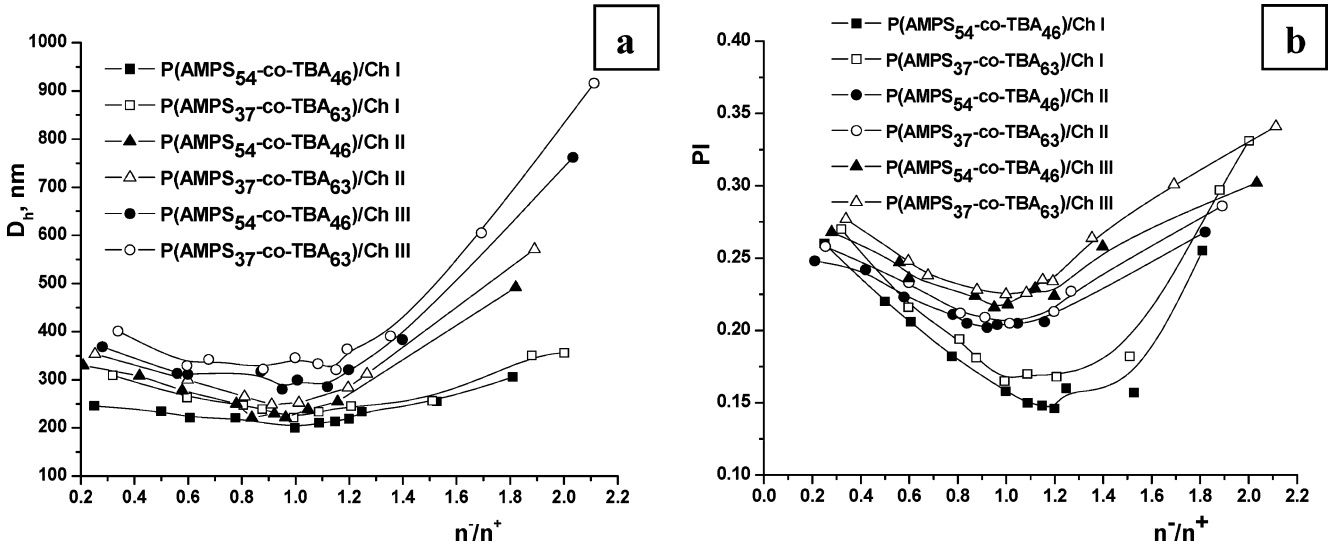

FIGURE 2. D_h (a) and PI (b) of the PEC dispersions as a function of the ratio between charges (n^-/n^+).

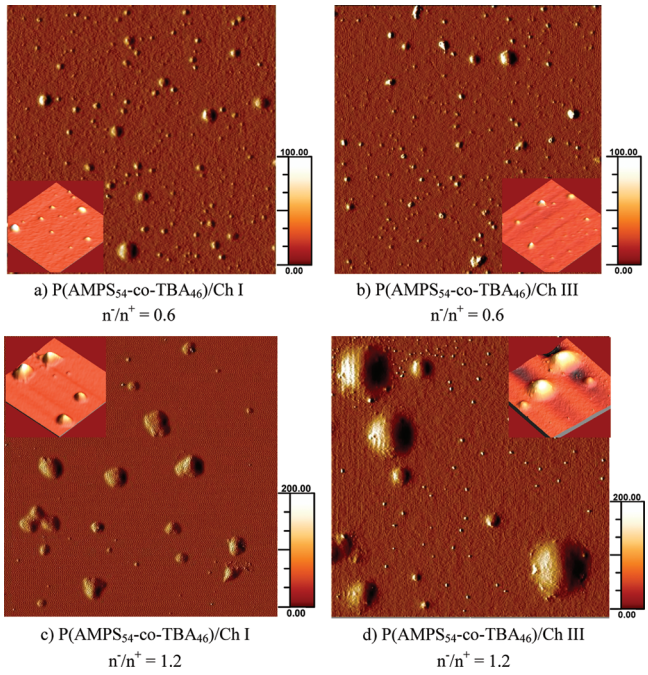

FIGURE 3. Tapping-mode-amplitude AFM images of the P(AMPS$_{54}$-*co*-TBA$_{46}$)/chitosan complex particles at different molar ratios between charges, adsorbed on the silicon wafers. The scan size was 5 × 5 μm^2 in all images. The insets show the 3D high AFM images of selected areas of the same samples; the scan size was 2 × 2 μm^2 in all images.

tions were used in the complex formation with P(AMPS-*co*-TBA) as polyanions (68), when PI was lower than 0.1.

The AFM amplitude images, obtained in the tapping mode, of some IPEC dispersions prepared in this work, with different molar ratios between charges, are presented in Figures 3 and 4.

As parts a and b of Figure 3 show, the AFM images indicated that before the stoichiometry ($n^-/n^+ = 0.6$), irrespective of the chitosan molar mass, the adsorbed dispersions appeared as small, individual, dispersed particles, when the IPECs were formed with P(AMPS$_{54}$-*co*-TBA$_{46}$) as the added polyion, whereas with P(AMPS$_{37}$-*co*-TBA$_{63}$) (Figure 4a), aggregated structures can be observed as dispersed between individual particles. Comparing Figure 3b with Figure 4a, one may note that the influence of the polyanion structure on the particle shape was stronger than that on their average size. The same characteristics were observed on different areas of the same sample, irrespective of the particle density on the surface (not shown here). Close to the stoichiometry, at $n^-/n^+ = 1.2$, the particle sizes strongly increased with an increase of the chitosan molar mass, for the same polyanion [P(AMPS$_{54}$-*co*-TBA$_{46}$) with ChI, Figure 3c, and with ChIII, Figure 3d]. When the shapes of IPECs formed with chitosan III and both copolymers (Figures 3d and 4b) are compared, the main difference consists of the presence of numerous very small particles like a corona around a condensed core for the complex particles formed with P(AMPS$_{37}$-*co*- TBA$_{63}$) (Figure 4b).

As was already mentioned, when the ratio between charges was increased, the particles size increased too, especially in the case of chitosan III. The AFM image in Figure 4c, corresponding to $n^-/n^+ = 1.8$, clearly shows an increase of the aggregation level between complex particles for the polyion pair P(AMPS$_{37}$-*co*-TBA$_{63}$)/chitosan III. For a better correlation of the results obtained in DLS analysis and the size observed in AFM images, Figure 4 includes also a graphical representation of the distribution of the particle sizes by number, obtained by DLS. As can be observed, the largest size distributions, with the particle sizes ranging between 300 and 1800 nm, were obtained for $n^-/n^+ = 1.8$ (Figure 4d). The DLS graphical representations corresponding to $n^-/n^+ = 0.6$ and 1.2 support the AFM images, indicating a decrease of the number of small particles with sizes lower than 200 nm by an increase of the molar ratio from 0.6 up to 1.2.

The particle sizes measured by DLS were compared with those in the dry state, measured by AFM, with the results being collected in Table 2.

As can be observed, the medium particle sizes of the complex nanoparticles measured by AFM were always lower than the average value measured by DLS, both before and

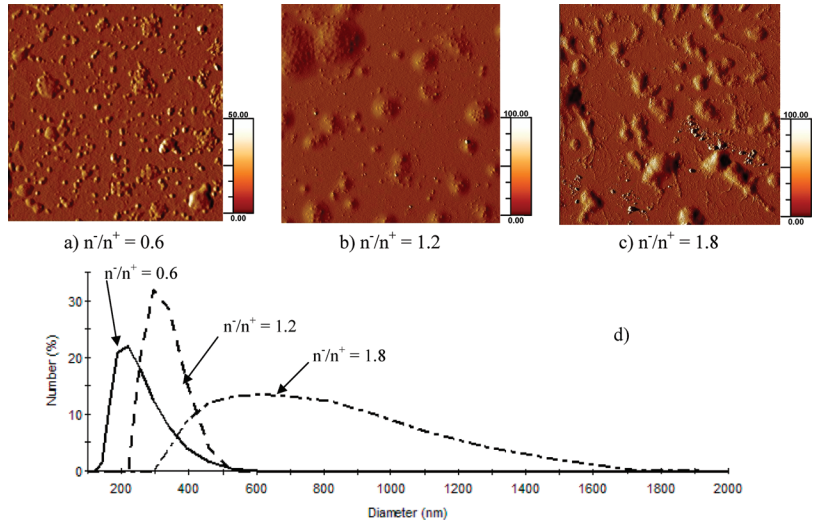

FIGURE 4. Tapping-mode-amplitude AFM images of the P(AMPS$_{37}$-*co*-TBA$_{63}$)/ChIII complex particles, at different molar ratios between charges (a–c), adsorbed on the silicon wafers. The scan size was 5 × 5 μm^2 in all images. DLS graphical representation of the particle size distribution by number (d).

Table 2. D_h Measured by DLS and Minimum (d_{min}), Medium (d_{med}), and Maximum (d_{max}) Diameters and the Medium *Z* Size (h_{med}) Determined by AFM for the Complex Particles Prepared from Some Polyion Pairs and Different Molar Ratios n^-/n^+

		DLS	AFM				
samples	n^-/n^+	D_h	d_{min}	d_{med}	d_{max}	h_{med}	Figures
P(AMPS$_{54}$-*co*-TBA$_{46}$)/ChI	0.6	222	22	158	579	98	2a, 3a
	1.2	231	27	219	651	186	2a, 3c
P(AMPS$_{54}$-*co*-TBA$_{46}$)/ChIII	0.6	281	22	213	519	122	2a, 3b
	1.2	272	29	257	877	202	2a, 3d
P(AMPS$_{37}$-*co*-TBA$_{63}$)/ChIII	0.6	337	22	216	611	161	2a, 4a
	1.2	359	44	315	509	277	2a, 4b
	1.8	691	57	581	1441	429	2a, 4c

after the complex stoichiometry. These differences were also evidenced for other systems (14, 68) and may be ascribed to the specificity of each method: AFM provides the size of dehydrated particles, and DLS measurements yield an ensemble average of the particle size in solution. Even if the interaction with the silica surface could induce conformational changes in the individual IPEC particles, because of electrostatic interactions during adsorption, after the air-drying procedure, the IPEC particles still display 3D structures (see the insets of Figure 3a–d), with almost spherical shapes. To sustain this characteristic, the values of the particle sizes in the *Z* axis, determined from AFM images, were also included in Table 2.

Compared to the image analysis of AFM micrographs, DLS is a very fast method to characterize dispersed particle sizes and distributions. However, DLS more easily detects large particles, and even a very small number of large particles lead to considerable changes in the obtained size distribution. Advantages of AFM are the direct evidence of the shape, size, and dispersity, which is not only an average value as that given by DLS. For instance, D_h determined for the complex particles of P(AMPS$_{37}$-*co*-TBA$_{63}$)/chitosan III, at

Scheme 2. Proposed Mechanism for the Formation of IPECs as Colloidal Dispersions from Chitosan as the Starting Polyions and P(AMPS-*co*-TBA) as the Added Polyions

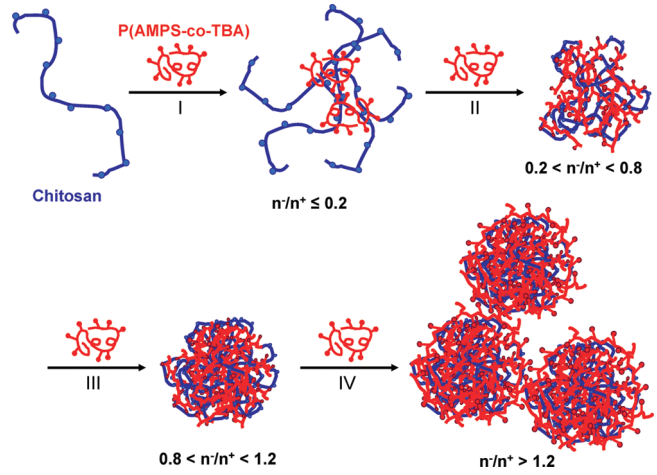

a molar ratio of 0.6, was 337 nm (Figure 2a and Table 2); when the AFM images obtained for the same polyion pair (Figure 4a) were analyzed, a much smaller medium diameter (216 nm, Table 2) was found because the *Particle Analysis* function of the device software measured all of the dispersed particles and also detected each particle that formed the bigger aggregates and sized them individually.

III.2. Mechanism of the Complex Formation between Chitosan and Random Copolymers of AMPS with TBA. Chitosan in a dilute solution (0.5 mM in this work) has a wormlike conformation (43, 44). Synthetic polyanions adopt a coiled conformation, as much as their concentration was 10 times higher than that of chitosan (5 mM). Therefore, in the complex formation between chitosan in excess and P(AMPS-*co*-TBA) polyanions, some peculiarities should be considered from the beginning. Thus, the charge density of the polyanions is about 0.5 for P(AMPS$_{54}$-*co*-TBA$_{46}$) and is much lower for P(AMPS$_{37}$-*co*-TBA$_{63}$). Furthermore, the nonionic comonomer, TBA, is hydrophobic,

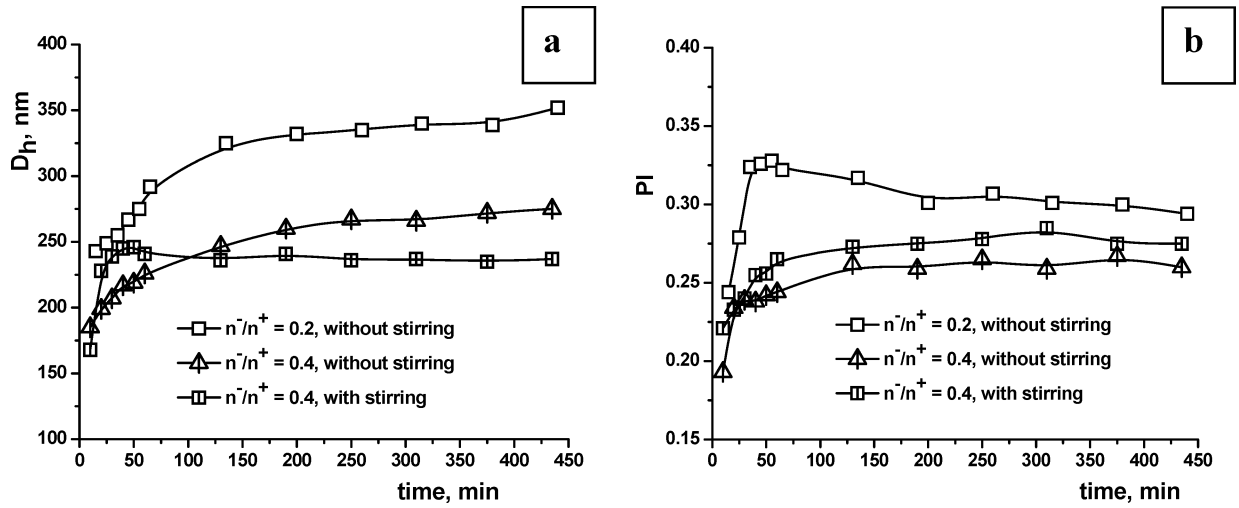

FIGURE 5. Particle sizes, D_h, and PI as a function of time for two molar ratios between charges for the polyion pair P(AMPS$_{54}$-*co*-TBA$_{46}$)/Ch I.

and some difficulties in the complex formation could be expected. Taking into account the DLS and AFM results, a mechanism in four steps has been assumed and presented in Scheme 2.

In the first step, the added polyanion interacts with chitosan chains, leading to the primary aggregates, which, taking into account the differences in the flexibility of the complementary polyions and the mismatch of charges, may contain more chitosan chains connected by fewer polyanion chains; such aggregates would have a high density of free positive charges compensated for with small counterions not by polyanion charges. The further addition of polyanion (step II, Scheme 2) led to the step-by-step neutralization of the positive charges of chitosan included in the primary aggregates, accompanied by rearrangements of chains and the formation of more compact particles with lower sizes. This assumption is supported by the monotonous decrease of the particle sizes with an increase of the molar ratio n^-/n^+ up to about 0.8 found by DLS measurements (Figure 2a). According to the literature, these particles have a "core–shell" structure characteristic for the formation of the IPECs as colloidal dispersions, with the level of aggregation being determined by the properties of polyelectrolytes (10, 14, 40, 43, 44, 68). For the polyion pairs investigated in this work, it was observed, both by DLS (Figure 2a) and AFM, that for n^-/n^+ ranging from about 0.8 up to 1.2 the particle sizes remained almost constant (step III, Scheme 2). As was already mentioned, the secondary aggregation would be not as fast as that in the case of flexible synthetic polycations. It seems that the ratio between charges of about 1.2 is a critical one for these systems, because an abrupt increase of the particle sizes and polydispersities was observed after this ratio (Figures 2a,b and 4d), supported also by the AFM images (Figure 4c) and sizes (Table 2) (step IV, Scheme 2).

Some kinetic data, D_h and PI as a function of time, for two molar ratios between charges, n^-/n^+, with chitosan I as the major component and P(AMPS$_{54}$-*co*-TBA$_{46}$) as the added polyion, are collected in Figure 5.

Figure 5a shows that the values of the particle sizes prepared at a lower ratio between charges, $n^-/n^+ = 0.2$, were higher than those prepared at $n^-/n^+ = 0.4$, with these results being in agreement with the mechanism presented in Scheme 2 and with the results presented in Figure 2a, when the particle sizes were measured after 24 h. The influence of stirring on the D_h values, in the first 60 min from the preparation of the complex dispersions, can be observed for the complex prepared at $n^-/n^+ = 0.4$. With stirring, the aggregation level fast increased in the first 60 min and leveled off after that; on the other hand, without stirring, a longer time was necessary for particles to reach the equilibrium at a higher value of D_h.

PI values (Figure 5b) abruptly increased in the first 25 min and slowly up to 125 min and remained almost constant after that up to 450 min, when the kinetics was followed for the sample corresponding to $n^-/n^+ = 0.4$, without stirring. The shape of the PI curve as a function of time was similar for the sample with stirring, only the values were a little higher. For the sample with $n^-/n^+ = 0.2$, without stirring, PI abruptly increased in the first 30 min and stabilized after 200 min to values higher than those found for $n^-/n^+ = 0.4$, sustaining thus the results presented in Figure 2b.

III.3. Colloidal Stability of the Chitosan-Based IPEC Dispersions. A very important characteristic of the IPECs as colloidal dispersions is their colloidal stability at storage. Therefore, the OD_{500} values and the particle sizes, D_h, measured after 24 h from preparation were compared with those measured after 1 week of storage. Parts a and b of Figure 6 illustrate the influence of the chitosan molar mass and of the polyanion structure on the OD_{500} values.

As can be observed in Figure 6a, the polyanion structure had a small influence on the stability of the IPEC dispersion before stoichiometry, when chitosan I was the starting polyion, but after stoichiometry, the complex formed with P(AMPS$_{37}$-*co*-TBA$_{63}$) exhibited a clear decrease of the turbidity, while the complex formed with the other polyanion was almost stable. When chitosan III was the starting polyion (Figure 6b), a very poor colloidal stability was observed after stoichiometry, indicated by the abrupt decrease of the OD_{500} values, for both polyanions. The same trend was observed

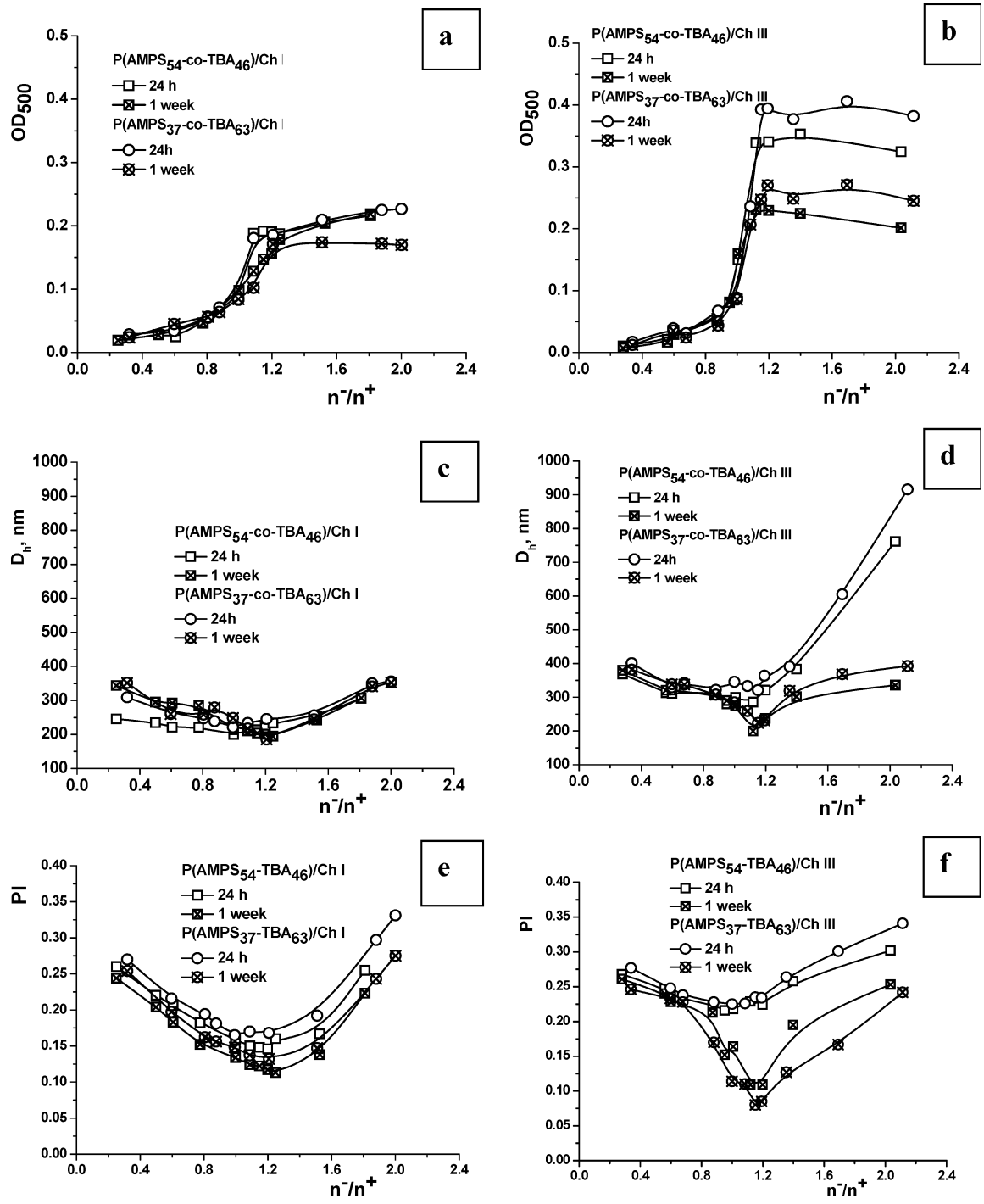

FIGURE 6. Storage colloidal stability of IPEC nanoparticles based on chitosan, at room temperature (22 °C), without stirring.

for the particle sizes and PI, with the highest colloidal stability, i.e., the lowest changes in the particle sizes and PI, being found in the case of chitosan with the lowest molar mass (chitosan I; Figure 6c,e) and the lowest colloidal stability in the case of chitosan with the highest molar mass (chitosan III; Figure 6d,f), mainly after stoichiometry. The lower storage stability shows that the bigger particles separated in time, with the measurements after 7 days being performed by collecting the supernatant, without stirring. The poor colloidal stability of the complex formed with chitosan III is a consequence of the highly aggregated structures observed by AFM at a molar ratio of 1.8 (Figure 4c).

III.4. Destabilization of a Model Suspension of Kaolin. A preliminary test of the efficiency of NIPEC dispersions in the destabilization of a kaolin model suspension compared with that of chitosan II was performed, with the results being collected in Figure 7.

Two samples of NIPECs were prepared starting from chitosan II with both polyanions, at a molar ratio, n^-/n^+, of

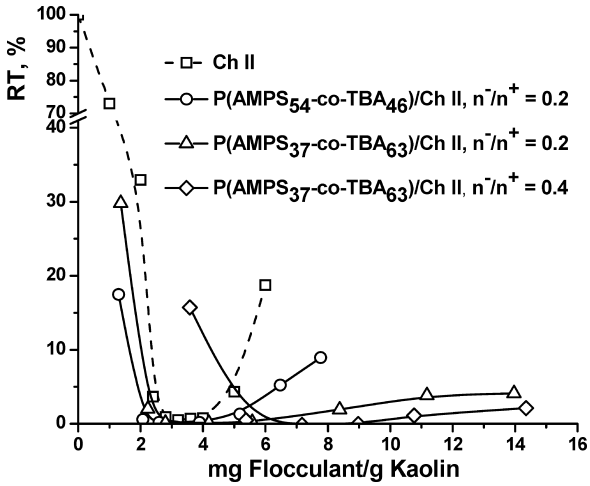

FIGURE 7. RT of a kaolin model suspension as a function the ratio between the amounts of flocculant and kaolin after destabilization with chitosan (Ch II) and nonstoichiometric polyelectrolyte complexes.

0.2. As Figure 7 shows, both samples of NIPEC dispersions were more efficient than chitosan in destabilization of the kaolin suspension, with a lower optimum flocculation concentration and a larger flocculation window being found, at the same time, compared with chitosan. The difference between the two complexes consists of a much larger flocculation window found for NIPEC prepared with P($AMPS_{37}$-*co*-TBA_{63}), i.e., with the higher content in a noionic comonomer. On the other hand, the NIPECs prepared with the same polyanion, at a molar ratio between charges of 0.4, led to a larger flocculation window than that with chitosan alone but also to a significant increase of the optimum flocculation concentration. The enlargement of the flocculation window, i.e., the higher concentration necessary for restabilization of the suspension compared with polycations, is a characteristic of the NIPECs as flocculants (24, 25). On the other hand, as was mentioned in the Introduction, the drawback of NIPECs as colloidal dispersions bearing free charges in excess, when they are used as flocculants, is the increase of the optimum flocculation concentration, which makes these flocculants not so cost-effective. With NIPECs prepared from chitosan at a ratio between charges of 0.2, it was demonstrated that this disadvantage could be overcome.

The optimum flocculation concentration lower than that found for chitosan supports the mechanism assumed in Scheme 2, according to which the complex aggregates formed at molar ratios up to 0.2 would possess a higher density of charges compensated for by small counterions and not involved in complexation.

IV. CONCLUSIONS

The formation of IPEC nanoparticles as colloidal dispersions from chitosan having molar masses of 470, 670, and 780 kDa and two ionic/nonionic random copolymers of AMPS with TBA was deeply investigated in the range of mixing molar ratios, n^-/n^+ of 0.15 up to 2.0, by the dropwise addition of the polyanion onto the chitosan. The decrease of the particle sizes up to the molar ratio between charges, n^-/n^+ of around 0.8, when chitosan was the major component, suggests that the addition of the polyanion onto chitosan led to both the formation of new particles, supported by the monotonous increase of the OD_{500} values, and also their rearrangement toward more compact structures. The region ranging from n^-/n^+ of 0.8 up to 1.2, characterized by an almost constant size of the complex particles, for all polyion pairs, seems to be a peculiarity of the chitosan-based complexes, taking into account the semirigid backbone of chitosan. The particle sizes were always higher when P($AMPS_{37}$-*co*-TBA_{63}) was the added polyion, i.e., for the polyanion with the highest content of hydrophobic comonomer.

The AFM images indicated that, before stoichiometry, the adsorbed particles appeared as small and individual particles, when the IPECs were formed with P($AMPS_{54}$-*co*-TBA_{46}) as the added polyion, irrespective of the chitosan molar mass, whereas highly aggregated structures were observed with P($AMPS_{37}$-*co*-TBA_{63}). A four-step mechanism was postulated for the formation of IPECs as colloidal dispersions from chitosan as the starting polyion and P($AMPS_{54}$-*co*-TBA_{46}) or P($AMPS_{37}$-*co*-TBA_{63}) as the added polyion. According to this mechanism, the primary aggregates formed at $n^-/n^+ \leq 0.2$ are larger than the particles formed at higher ratios between charges and would have a high density of free positive charges, noninvolved in complexation with polyanion, which makes them more effective than chitosan in destabilization of a kaolin model suspension. The higher the content of TBA in polyanion was, the larger the flocculation window, with the optimum concentration of flocculant being also lower compared with that of chitosan.

Acknowledgment. The authors are thankful for financial support provided by the Saxon Ministry of Sciences and Fine Arts and the European Project Romanian Action for Integrating, Networking and Strengthening the ERA (RAINS).

REFERENCES AND NOTES

(1) Michaels, A. S. *Ind. Eng. Chem.* **1965**, *57*, 32–40.
(2) Tsuchida, E.; Abe, K. *Adv. Polym. Sci.* **1982**, *45*, l–119.
(3) Philipp, B.; Dautzenberg, H.; Linow, K. J.; Kötz, J.; Dawydoff, W. *Prog. Polym. Sci.* **1989**, *14*, 91–172.
(4) Michaels, A. S.; Miekka, R. G. *J. Phys. Chem.* **1961**, *65*, 1765–1773.
(5) Dautzenberg, H. *Macromolecules* **1997**, *30*, 7810–7815.
(6) Dragan, S.; Cristea, M. In *Recent Research Developments in Polymer Science*; Gayathri, A., Ed.; Research Signpost: Trivandrum, India, 2003; Vol. 7, pp 149–181.
(7) Kabanov, V. A.; Zezin, A. B. *Pure Appl. Chem.* **1984**, *56*, 343–354.
(8) Kabanov, V. A.; Kabanov, A. V. *Macromol. Symp.* **1995**, *98*, 601–613.
(9) Anderson, T.; Holappa, S.; Aseyev, V.; Tenhu, H. *J. Polym. Sci., Part A: Polym. Chem.* **2003**, *41*, 1904–1914.
(10) Buchhammer, H.-M.; Petzold, G.; Lunkwitz, K. *Langmuir* **1999**, *15*, 4306–4310.
(11) Gärdlundm, L.; Wågberg, L.; Gernandt, R. *Colloids Surf. A* **2003**, *218*, 137–149.
(12) Nyström, R. G.; Rosenholm, J. B.; Nurmi, K. *Langmuir* **2003**, *19*, 3981–3986.
(13) Chen, J.; Heitmann, J. A.; Hubbe, M. A. *Colloids Surf. A* **2003**, *223*, 215–230.
(14) Müller, M.; Kessler, B.; Richter, S. *Langmuir* **2005**, *21*, 7044–7051.
(15) Paneva, D.; Mespouille, L.; Manolova, N.; Degée, P.; Rashkov, I.; Dubois, P. *J. Polym. Sci., Part A: Polym. Chem.* **2006**, *44*, 5468–5479.
(16) Buchhammer, H.-M.; Mende, M.; Oelmann, M. *Colloids Surf. A* **2003**, *218*, 151–159.
(17) Gummel, J.; Boué, F.; Demé, B.; Cousin, F. *J. Phys. Chem. B* **2006**, *110*, 24837–24846.

(18) Hartig, S. M.; Carlesso, G.; Davidson, J. M.; Prokop, A. *Biomacromolecules* **2007**, *8*, 265–272.
(19) Petzold, G.; Nebel, A.; Buchhammer, H.-M.; Lunkwitz, K. *Colloid Polym. Sci.* **1998**, *276*, 125–130.
(20) Reihs, T.; Müller, M.; Lunkwitz, K. *J. Colloid Interface Sci.* **2004**, *271*, 69–79.
(21) Sui, Z.; Jaber, J. A.; Schlenoff, J. B. *Macromolecules* **2006**, *39*, 8145–8152.
(22) Oupicky, D.; Parker, A. L.; Seymour, L. W. *J. Am. Chem. Soc.* **2002**, *124*, 8–9.
(23) Laue, C.; Hunkeler, D. *J. Appl. Polym. Sci.* **2006**, *102*, 885–896.
(24) Schwarz, S.; Dragan, E. S. *Macromol. Symp.* **2004**, *210*, 185–192.
(25) Mende, M.; Schwarz, S.; Petzold, G.; Jaeger, W. *J. Appl. Polym. Sci.* **2007**, *103*, 3776–3784.
(26) Renault, F.; Sancey, B.; Badot, P.-M.; Crini, G. *Eur. Polym. J.* **2009**, *45*, 1337−1348.
(27) Xiang, F.; Cheng, G.; Yi, K.; Ma, L. *J. Appl. Polym. Sci.* **2005**, *96*, 2225–2229.
(28) Chellat, F.; Tabrizian, M.; Dumitriu, S.; Chornet, E.; Magny, P.; Rivard, C.-H.; Yahia, L'H. *J. Biomed. Mater. Res.* **2000**, *51*, 107–116.
(29) Yao, K. D.; Tu, H.; Cheng, F.; Zhang, J. W.; Liu, J. *Angew. Makromol. Chem.* **1997**, *245*, 63–72.
(30) Sakiyama, T.; Chu, C.-H.; Fujii, T.; Yano, T. *J. Appl. Polym. Sci.* **1993**, *50*, 2021–2025.
(31) Gamzazade, A. I.; Nasibov, S. M. *Carbohydr. Polym.* **2002**, *50*, 339–343.
(32) Yi, H.; Wu, L.-Q.; Bentley, W. E.; Ghodssi, R.; Rubloff, G. W.; Culver, J. N.; Payne, G. F. *Biomacromolecules* **2005**, *6*, 2881–2894.
(33) Kenawy, E.-R.; Worley, S. D.; Broughton, R. *Biomacromolecules* **2007**, *8*, 1359–1384.
(34) Ravi Kumar, M. N. V.; Muzzarelli, R. A. A.; Muzzarelli, C.; Sashiva, H.; Domb, A. J. *Chem. Rev.* **2004**, *104*, 6017–6084.
(35) Bratskaya, S.; Schwarz, S.; Laube, J.; Liebert, T.; Heinze, T.; Krentz, O.; Lohmann, C.; Kulicke, W. M. *Macromol. Mater. Eng.* **2005**, *290*, 778–785.
(36) Bratskaya, S.; Avramenko, V.; Schwarz, S.; Philippova, I. *Colloids Surf. A* **2006**, *275*, 168–176.
(37) Cerrai, P.; Guerra, G. D.; Tricoli, M. *Macromol. Chem. Phys.* **1996**, *197*, 3567–3579.
(38) Nge, T. T.; Yamaguchi, M.; Hori, N.; Takemura, A.; Ono, H. *J. Appl. Polym. Sci.* **2002**, *83*, 1025–1035.
(39) Stoilova, O.; Koseva, N.; Manolova, N.; Rashkov, I. *Polym. Bull.* **1999**, *43*, 67–73.
(40) de Vasconcelos, C. L.; Bezerril, P. M.; dos Santos, D. E. S.; Dantas, T. N. C.; Pereira, M. R.; Fonseca, J. L. C. *Biomacromolecules* **2006**, *7*, 1245–1252.
(41) Fukuda, H.; Kikuchi, Y. *Makromol. Chem.* **1979**, *180*, 1631–1633.
(42) Kikuchi, Y.; Noda, A. *J. Appl. Polym. Sci.* **1976**, *20*, 2561–2562.
(43) Schatz, C.; Lucas, J. M.; Viton, C.; Domard, A.; Pichot, C.; Delair, T. *Langmuir* **2004**, *20*, 7766–7778.
(44) Drogoz, A.; David, L.; Rochas, C.; Domard, A.; Delair, T. *Langmuir* **2007**, *8*, 10950–10958.
(45) Kubota, N.; Kikuchi, Y. In *Structural Diversity and Functional Versatility of Polysaccharides*; Dumitriu, S., Ed.; Marcel Dekker Inc.: New York, 1998; pp 595−628.
(46) Liu, W. G.; Yao, K.; Liu, Q. G. *J. Appl. Polym. Sci.* **2001**, *82*, 3391–3395.
(47) Mi, F.-L.; Shyu, S.-S.; Wong, T. B.; Jang, S.-F.; Lee, S.-T.; Lu, K.-T. *J. Appl. Polym. Sci.* **1999**, *74*, 1093–1107.
(48) Shi, X.; Du, Y.; Sun, L.; Zhang, B.; Dou, A. *J. Appl. Polym. Sci.* **2006**, *100*, 4614–4622.
(49) Yan, X.-L.; Khor, E.; Lim, L.-Y. *J. Biomed. Mater. Res. (Appl. Biomater.)* **2001**, *58*, 358–365.
(50) Wang, L.; Khor, E.; Wee, A.; Lim, L.-Y. *J. Biomed. Mater. Res. (Appl. Biomater.)* **2002**, *63*, 610–618.
(51) Lee, K. Y.; Park, W. H.; Ha, W. S. *J. Appl. Polym. Sci.* **1997**, *63*, 425–432.
(52) Kang, H.-S.; Park, S.-H.; Lee, Y.-G.; Son, T.-I. *J. Appl. Polym. Sci.* **2007**, *103*, 386–394.
(53) Zintchenko, A.; Dautzenberg, H.; Tauer, K.; Khrenov, V. *Langmuir* **2002**, *18*, 1386–1393.
(54) Mun, G. A.; Khutoryanskiy, V. V.; Nurkeeva, Z. S.; Sergaziyev, A. D.; Fefelova, N. A.; Rosiak, J. M. *J. Polym. Sci., Part B: Polym. Phys.* **2004**, *42*, 1506–1513.
(55) Kono, K.; Okabe, H.; Morimoto, K.; Takagishi, T. *J. Appl. Polym. Sci.* **2000**, *77*, 2703–2710.
(56) Gao, Y.; Chen, X.; Liao, B.; Ding, X.; Zheng, Z.; Cheng, X.; Pang, H.; Peng, Y. *Polym. Bull.* **2006**, *56*, 305–311.
(57) Indirect food additives: adhesives and components of coatings [http://www.accessdata.fda.gov/scripts/cdrh/cfdocs/cfcfr/CFRSearch.cfm?CFRPart=175&showFR=1&subpartNode=21:3.0.1.1.6.2].
(58) Liu, H. Y.; Zhu, X. X. *Polymer* **1999**, *40*, 6985–6990.
(59) Ozturc, V.; Okay, O. *Polymer* **2002**, *43*, 5017–5026.
(60) Gamzazade, A. I.; Shimac, V. M.; Skljar, A. M.; Stykova, E. V.; Pavlova, S. A.; Rogozin, S. V. *Acta Polym.* **1985**, *36*, 420–424.
(61) Brugnerotto, J.; Lizardi, J.; Goycoolea, F. M.; Argüelles-Monal, W.; Desbriéres, J.; Rinaudo, M. *Polymer* **2001**, *42*, 3569–3580.
(62) Dragan, E. S.; Mihai, M.; Schwarz, S. *Colloids Surf. A* **2006**, *290*, 213–221.
(63) Koppel, D. E. *J. Chem. Phys.* **1972**, *57*, 4814–4820.
(64) Pavlath, A. E.; Wong, D. W. S.; Robertson, G. H. In *Polymeric Materials Encyclopedia*; Salamone, J. S., Ed.; CRC Press: New York, 1996; Vol. 2, pp 1230−1234.
(65) Schatz, C.; Pichot, C.; Delair, T.; Viton, C.; Domard, A. *Langmuir* **2003**, *19*, 9896–9903.
(66) Boucard, N.; David, L.; Rochas, C.; Montembault, A.; Viton, C.; Domard, A. *Biomacromolecules* **2007**, *8*, 1209–1217.
(67) Dragan, E. S.; Schwarz, S. *J. Polym. Sci., Part A: Polym. Chem.* **2004**, *42*, 5244–5252.
(68) Mihai, M.; Dragan, E. S.; Schwarz, S.; Janke, A. *J. Phys. Chem. B* **2007**, *111*, 8668–8675.

AM900109U